

Endoscopic Lumbar Disc Surgery

Essay

Submitted in Partial Fulfillment of the Master Degree
in General surgery

By

Abd-Elgalel Ragab Abd-Elgalel

(M.B.B.Ch)

Resident of neurosurgery

Faculty of Medicine – AL Azhar University

Supervised By

Prof. Dr. Elsayed Abd-Elrahman Ibrahim Elmor

Professor of Neurosurgery

Faculty of Medicine – AL Azhar University

Prof. Dr. Mohammed Salah Al-din Shehata

Professor of General surgery

Faculty of Medicine – AL Azhar University

Dr. Mustafa Hassan Alwalily

Assistant Professor of Neurosurgery

Faculty of Medicine – AL Azhar University

Dr. Adel Ragab Al Melisy

Lecturer of Neurosurgery

Faculty of Medicine – AL Azhar University

Faculty of medicine

Al-Azhar University

2013

استئصال الغضروف القطني بواسطة المنظار الجراحي

رسالة

توطئه للحصول على درجة الماجستير في الجراحة العامة

مقدمة من

الطبيب/ عبد الجليل رجب عبد الجليل
بكالوريوس الطب والجراحة
طبيب مقيم بقسم جراحة المخ والأعصاب

اشراف

أ.د/ السيد عبد الرحمن إبراهيم المر

أستاذ جراحة المخ والأعصاب
كلية الطب - جامعة الأزهر

أ.د/ محمد صلاح الدين شحاتة

أستاذ الجراحة العامة
كلية الطب - جامعة الأزهر

أ.د/ مصطفى حسن الوليلي

أستاذ مساعد جراحة المخ والأعصاب
كلية الطب - جامعة الأزهر

د./ عادل رجب المليسي

مدرس جراحة المخ والأعصاب
كلية الطب - جامعة الأزهر

كلية الطب جامعة الأزهر

٢٠١٣

بِسْمِ اللَّهِ الرَّحْمَنِ الرَّحِيمِ

(قَالُوا سُبْحَانَكَ لَا عِلْمَ لَنَا إِلَّا هَا

عَلَّمْتَنَا إِنَّكَ أَنْتَ الْعَلِيمُ

الْحَكِيمُ)

صَدَقَ اللَّهُ الْعَظِيمُ

CONTENTS

<i>SUBJECT</i>	<i>PAGE NO</i>
<i>INTRODUCTION</i>	1
<i>AIM OF THE WORK</i>	3
<i>DEVELOPMENTAL SPINAL ANATOMY</i>	4
<i>ANATOMY OF LUMBAR SPINE</i>	14
<i>BIOMECHANICS</i>	41
<i>PATHOPHYSIOLOGY OF LUMBAR DISC HERNIATION...</i>	51
<i>CLINICAL PRESENTATION OF LUMBAR DISC HERNIATION</i>	54
<i>INVESTIGATION OF LUMBAR DISC HERNIATION</i>	61
<i>SURGICAL MANAGEMENT</i>	70
<i>SUMMARY</i>	106
<i>REFERENCES</i>	108
<i>ARABIC SUMMARY</i>	--

LIST OF TABLES

<i>Subject</i>	<i>Page No</i>
Table (1): Clinical characteristics of 150consecutive microendoscopic discectomy patients.....	90
Table (2): Modified Macnab criteria used to assess clinical outcome in 150 consecutive patients undergoing microendoscopic discectomy.....	91
Table (3): Mean operative times, complications, mean hospital stay, and mean time to return to work for 150 consecutive patients undergoing microendoscopic discectomy	91

LIST OF FIGURES

<i>SUBJECT</i>	<i>PAGE NO</i>
Figure (I-1): Formation of bilaminar germ disc from the embryoblast. The epiblast is adjacent to the amniotic cavity, and the hypoblast is adjacent to the blastocyst cavity.	5
Figure (I.2): Formation of neural tube and dorsal root ganglion (axial view). A, Elevation of ectoderm creates neural folds that invaginate and ultimately fuse to form a neural tube. B, Neural crest cells form from lateral edges of these neuroectodermal cells, migrate toward the underlying mesoderm, and give rise to cranial nerve ganglia, spinal ganglia, and dorsal root ganglia (DRG).	5
Figure (I-3): Sagittal representation showing initial stages of formation of notochord. The notochordal process becomes canalized and breaks through the caudal aspect of the ectoderm. This allows transient communication between the yolk sac and the amniotic cavity through the neurenteric canal.	5
Figure (I. 4): Conversion of somite to sclerotome and dermatomyotome (axial view). The paraxial mesoderm organizes into segments called somitomeres, which subsequently become somites beginning by approximately day 20. Each somite undergoes further specialization into the sclerotome, myotome, and dermatome by the beginning of the fourth week. A portion of the sclerotome surrounds the notochord and becomes the vertebral body and posterior elements. The dorsolateral aspect of the somite forms the dermomyotome, which differentiates into the myotome medially and the dermatome laterally. The dermatomes give rise to the dermis of the neck, back, and ventral and lateral trunk, and the myotomes form the deep back muscles and abdominal muscles.	8
Figure (I. 5): Coronal representation of formation of the vertebral column from adjacent sclerotome segments. A, Each sclerotome is divided by sclerotomic fissure into a cranial and a caudal portion. The cranial half of one sclerotome segment fuses with the caudal half of the adjoining segment, ultimately giving rise to the primordium of the vertebral body (centrum). B, Some of the notochordal tissue eventually disappears, whereas other notochordal cells remain and become the precursor of the intervertebral disc. The segmental nerve, which was originally located at the center of the sclerotome, comes to lie between adjacent centra, opposite the intervertebral disc. The segmental vessels come to lie over the middle of the centrum.	9

<i>SUBJECT</i>	<i>PAGE NO</i>
Figure (I.6): Schematic representation of mammalian vertebrae development. (A), Notochord is surrounded by axial mesenchyme with the segmental vessels located between adjacent sclerotomes. The dermomyotome forms from the dorsolateral aspect of the somite. (B), Differentiation of axial mesenchyme into dense perichordal disc, which becomes the intervertebral disc, and loose perichordal disc, which becomes the centrum. The costal element is located lateral to the future intervertebral disc. Note the relationship of the segmental vessels to the future centrum: they originally lie between adjacent sclerotomes but ultimately come to lie at the mid-point of the centrum, which is composed of cranial and caudal portions of adjacent sclerotomes. (C), Differentiation of notochord into the mucoid streak and the nucleus pulposus. The notochordal cells at the center of the dense perichordal disc persist as the precursor of the future intervertebral disc (nucleus pulposus).	11
Figure (I. 7): Developmental stages of a typical vertebra: membranous (A), chondrification (B), ossification (C), and at birth (D). The sclerotome that surrounds the notochord forms the membranous vertebral column. This is converted to a cartilaginous model via the process of chondrification, in which the cartilaginous centrum is formed by two centers and each half of the neural arch is formed by one center. Each costal process is chondrified separately.	13
Figure (II. 1): Lumbar vertebra superior view.	17
Figure (II. 2): 3 rd and 4th lumbar vertebrae: posterior view.	18
Figure (II. 3): Left lateral view (partially sectioned).	20
Figure (II. 4): Intervertebral disc.	22
Figure (II. 5): Spinal nerve roots exit.	24
Figure (II. 6): Endoscopic view showing the thoracolumbar fascia as an avascular heavy band of interwoven fibers.	28
Figure (II. 7): The paravertebral muscles of the lumbar spine are seen as a moderately vascular muscle bundle.	28
Figure (II. 8): Illustration of triangular working zone: A, exiting root that forms anterior boundary of triangular working zone; B, triangular working zone; C, traversing root.	29
Figure (II. 9): Endoscopic view of annular surface in triangular working zone. Note the loose/woven adipose tissue on the surface of annulus.	29

<i>SUBJECT</i>	<i>PAGE NO</i>
Figure (II. 10): Intraoperative photo demonstrating presence of superficial veins on surface of annulus.	30
Figure (II. 11): Endoscopic view of content of spinal canal (A) and herniated lumbar disc(B).	33
Figure (II. 12): Photograph demonstrating arteries and venous system of nerve root and A.V. anastomosis.	34
Figure (II. 13): Illustration showing origin of segmental arteries of lumbar spine.	34
Figure (II. 14): Ligamentous structures of ventral dura and nerve root.	36
Figure (II. 15): Gross anatomy of annulus fibrosus and NP in young cadaver specimen. Thenucleus has been injected with methylene blue. Note, however, the thickness of the annulusfibrosus anteriorly and posterolaterally.	37
Figure (II. 16): Endoscopic view of NP in a 45-yr-old male following interdiscal injection of diluted indigo carmine. Note the unstained partially collagenized nucleus mixed with stained soft nuclear tissue.	38
Figure (II. 17): Endoscopic view of capsular ligamentum flavum complex, which appears as an avascular structure.	40
Figure (II. 18): View of ventral surface of posterior longitudinal ligamentum (PLL).	40
Figure (III. 1): Eccentrically borne load results in annulus fibrosus bulging on the concave side of the resultant spinal curve, and annulus fibrosus tension is present on the convex side of the curve. Nucleus pulposus, however, tends to move in the opposite direction as the annulus fibrosus bulge when an eccentric load is borne (solid to dashed outline).	46
Figure (III. 2): Ligaments and their effective moment arms. Note that this length depends on the location of the instantaneous axis of rotation (®). An "average" location is used in this illustration. ALL indicates anterior longitudinal ligament; PLL, posterior longitudinal ligament; LF, ligamentum flavum; CL, capsular ligament; ISL, interspinous ligament.	48
Figure (VI. 1): Myelogram lat. film showing L ₄₋₅ disc	68
Figure (VI. 2): Non contrast axial CT showing left posterolateral L ₄₋₅ disc prolapse.	68

<i>SUBJECT</i>	<i>PAGE NO</i>
Figure (VII. 1): MED system of dilators, K-wire, tubular retractor, and flexible arm assembly.	75
Figure (VII. 2): Standard video equipment used for the MED procedure.	75
Figure (VII. 3): Endoscopic assembly for the MED system.	76
Figure (VII.4): Instruments used to perform MED procedure. Bayoneted instruments and a long, thin, tapered drill simplify the procedure.	77
Figure (VII.5): Operating room set-up for MED procedure. Fluoro, fluoroscopy.	78
Figure (VII. 6): A , illustrations showing initial dilator in place sweeping paraspinal musculature off lamina, B , sequential dilators for muscle splitting approach, and C , tubular retractor with endoscope in place.	81
Figure (VII 7): Illustration of endoscopic image on the video monitor showing the initial image orientation to be incorrect (A) Proper orientation is achieved by turning the gold ring on the endoscopic assembly so that the V-shaped indicator (B) is in the same position on the video monitor as the endoscope is within the tubular retractor. At completion (C), the medial anatomy is at 12 o'clock and the lateral anatomy is at 6 o'clock on the video screen to give the surgeon proper orientation for performing MED.	83
Figure (VII.8): (A) hemilaminotomy being preformed with a Kerrison punch, (B) removal of ligamentum flavum with up-going curette, (C) exposure of dura and traversing nerve root, and (D) removal of disc herniation under retracted nerve root.	86
Figure (VII .9): Patient outcomes as defined by the modified MacNab criteria showing data from 150 consecutive cases performed using the MED system.	92
Figure (VII. 10): A , the spinolaminar junction target for localization is highlighted. B , a fluoroscopically guided percutaneous Steinman pin is placed at this target.	96
Figure (VII.11): Serial dilators are sequentially placed to dilate the dorsal musculature and fascia. This process is confirmed by lateral fluoroscopy (inset).	97
Figure (VII.12): Working channel and endoscope docked in place with drilling of the bony lamina	98
Figure (VII.13): A , a small, angled curette used to define the laminar edge. B , Kerrison punches and drills are used to continue the bony decompression.	99
Figure (VII.14): A , the working channel and endoscope are angled to provide a wide contralateral view. B , this allows for a near circumferential decompression of the central spinal canal to the level of the contralateral lateral recess	100
Figure (VII. 15): Summary of the outcome by clinical symptoms (Sx) between the MEDL and open-surgery groups. Dist, distance.	105

INTRODUCTION

Virchow first described traumatic lumbar intervertebral disc disease in 1857. Contributions from physicians striving to understand back pain and sciatica have encouraged the development of new surgical interventions, as well as conservative modalities, for the treatment of spinal disorders. In 1955, Malis began using a binocular microscope, in conjunction with bipolar coagulation, to aid his surgical approach. After the introduction of the intraoperative use of an operating microscope for discectomies, Yasargil and Caspar introduced the minimally invasive concept of microdiscectomy. In 1975, Hijikata described the first percutaneous endoscopic discectomy. In 1983, Kambin and Gellman performed a discectomy by inserting a Craig cannula and a small forceps into the disc space, after an open laminectomy, evacuate the nucleus pulposus (**Guiot BH et al., 2002**).

There are many applications of endoscopy in spine surgery including; endoscopic discectomy for lumbar disc herniation, microendoscopic decompression for treatment of lumbar stenosis, laparoscopic anterior lumbar interbody fusion, minimally invasive percutaneous posterior lumbar interbody fusion (**Kafadar et al., 2006**).

Minimal invasive endoscopic spinal surgery has numerous advantages including ; reduced operative time; less soft tissue damage; reduced muscle splitting and retraction; less postoperative

pain; reduced blood loss; faster recovery; and shorter hospital stay (*Choi G et al., 2007*).

Complications of endoscopic spinal surgery can be related to anesthesia, patient positioning, and surgical technique (*Yeung et al., 2006*).

Complications related to surgical technique include; dural tear with a delayed pseudomeningocele formation, discitis, due to scraping of the end plates by the automated nucleotome during disc removal, and cauda equina injury. However, once mastered, endoscopic spinal procedures can result in a significant reduction of complications and postoperative pain and discomfort and return patients to their daily life activities sooner than standard open, more conventional procedures (*Brayda-Bruno et al., 2006*).

The performance of successful minimally invasive endoscopic spinal surgery is beset with several technical challenges, including the limited tactile feedback, two-dimensional video image quality of three-dimensional anatomy, and the manual dexterity needed to manipulate instruments through small working channels (*Yeung et al., 2006*).

The success of endoscopic spine surgery hinges on the proper patient selection, for example the inclusion criteria for endoscopic lumbar discectomy are similar to the well-known indications for open laminectomy and discectomy; Failure to respond to nonoperative conservative measures, presence of positive tension signs, correlative

dermatomal distribution of sciatic pain, and correlative positive imaging studies (*Ruetten et al., 2005*).

Exclusion criteria for endoscopic disc surgery include low back pain due to degenerative disc process, also cauda equina syndrome as it is usually associated with some degree of bony and ligamentous abnormality. Individuals with a global bulging disc and sciatica are usually suffering from spinal stenosis; they are best treated by open procedures. A sequestered disc, which has migrated in a cephalad or caudal direction in the spinal canal, will require laminectomy for the retrieval of herniated fragments (*Gupta et al., 2007*).

AIM OF THE WORK

The aim of this work is to review the current concepts in endoscopic lumbar spine surgery regarding; endoscopic anatomy of the spine, applications, advantages, inclusion criteria, exclusion criteria, types of endoscopes & instruments used, surgical techniques, complications and lastly the future of minimal invasive endoscopic lumbar spine surgery.

DEVELOPMENTAL SPINAL ANATOMY

The preembryonic period (weeks 0 To 3)

The preembryonic period. Which begins at fertilization and continues for approximately 3 weeks, is characterized by the development of the bilaminar germ disc (Fig. I. 1). The bilaminar germ disc is converted to the trilaminar germ disc during the next stage, the embryonic period. (*Sadler T.W. 2000*)

The embryonic period (weeks 3 to 8)

The third week of gestation is characterized by the processes of gastrulation and neurulation. Gastrulation is the process of the formation of all three embryonic germ layers : ectoderm , mesoderm , and endoderm.

Neurulation, which is initiated in the latter half of the third week. Is a process of folding that converts the neural plate, a thickening of the ectoderm overlying the notochord, to the neural tube (Fig I. 2) (*Larsen W.J. 2001*)

Notochord

From the primitive pit, a rod-like process of cells called the notochordal process moves cranially up to the prechordal plate by day 20. The notochordal process, which is the precursor of the skeletal axis, becomes canalized and caudally breaks through the ectodermal surface at the primitive node. The tube then opens ventrally starting at the level of the pit and proceeds cephalad. The yolk sac therefore transiently communicates with the amniotic cavity through the opening at the pit called the neurenteric canal (Fig. I. 3). After the tube opens, it is converted to a central ventral bar of mesoderm called the notochordal plate, which detaches from the endoderm by day 22 to 24 and becomes entirely contained within the mesoderm. It then forms a solid cylinder of cells to form the definitive notochord (*Sadler T. W. 2000*).

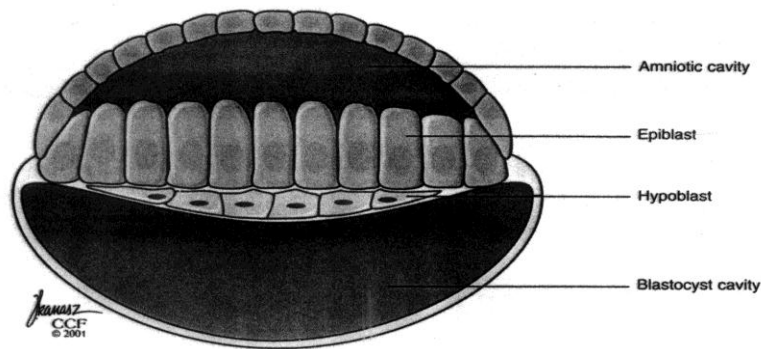


Figure (I-1): Formation of bilaminar germ disc from the embryoblast. The epiblast is adjacent to the amniotic cavity, and the hypoblast is adjacent to the blastocyst cavity. (Courtesy Cleveland Clinic, Division of Education, © 2001.)

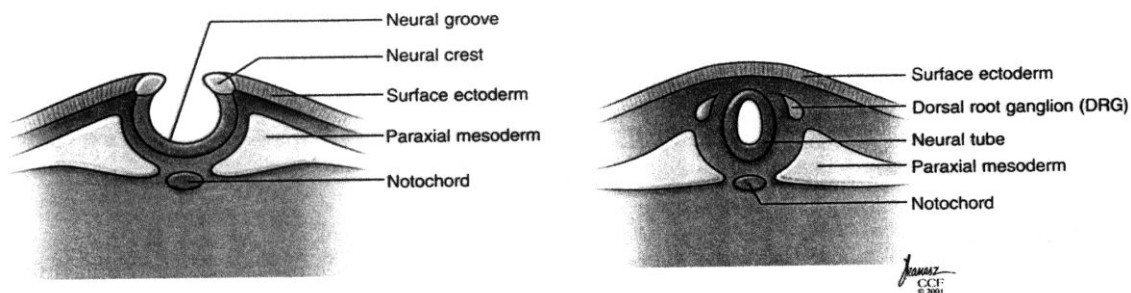


Figure (I.2): Formation of neural tube and dorsal root ganglion (axial view). A, Elevation of ectoderm creates neural folds that invaginate and ultimately fuse to form a neural tube. B, Neural crest cells form from lateral edges of these neuroectodermal cells, migrate toward the underlying mesoderm, and give rise to cranial nerve ganglia, spinal ganglia, and dorsal root ganglia (DRG). (Courtesy Cleveland Clinic, Division of Education, ©2001.)

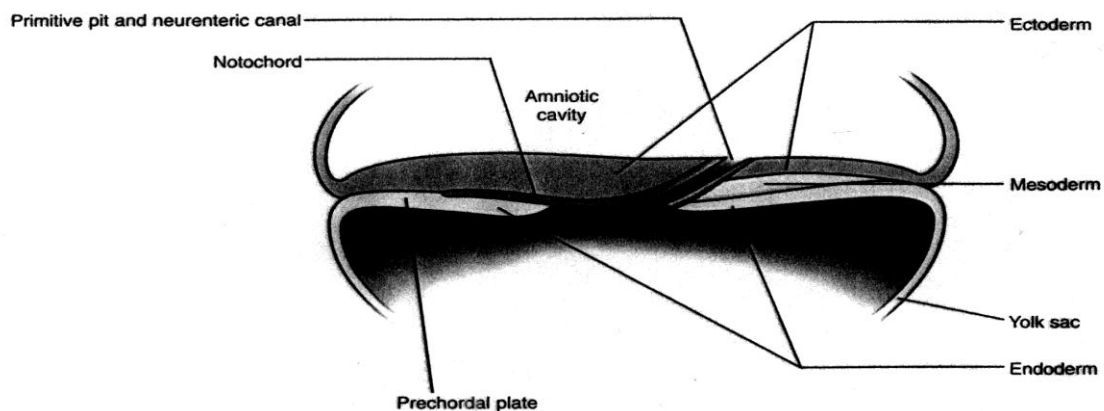


Figure (I-3): Sagittal representation showing initial stages of formation of notochord. The notochordal process becomes canalized and breaks through the caudal aspect of the ectoderm. This allows transient communication between the yolk sac and the amniotic cavity through the neurenteric canal. (Courtesy Cleveland Clinic, Division of Education, ©2001.)

Neurulation

At the initiation of neurulation, the notochord and prechordal mesoderm cause the overlying ectoderm to thicken and to form the neural plate. This tongue-shaped structure elongates gradually toward the primitive streak, and by the end of the third week, the lateral edges of this plate become elevated to form the neural folds, which surround the neural groove. The neural folds fuse in the midline in the region of the embryo's future neck. The fusion gradually proceeds cephalad and caudal, thereby forming the neural tube. The two ends of the neural tube communicate with the amniotic cavity through openings called neuropores. The cranial neuropore closes by approximately day 25, and the caudal neuropore closes by approximately day 27. Neurulation is then completed. The closed neural tube has a narrow caudal portion representing the future spinal cord and a broad cephalic portion, with a number of dilatations called brain vesicles, representing the future brain. (*Moore K.L. et al, 2002*)

Paraxial mesoderm

Along the length of the notochord, the mesenchyme becomes organized into three zones: the medial paraxial mesoderm, a narrower intermediate mesoderm, and the flattened lateral plate mesoderm. By the beginning of the third week, the paraxial mesoderm is organized into segments called somitomeres. The segmentation proceeds cephalocaudally. In the cephalic region, the somitomeres in association with neural plate segmentation, form neuromeres, which contribute most of the head mesenchyme. By day 20, somitomeres organize into somites, starting in the cervical region and proceeding at a rate of three pairs per day. By the end of week 5, there are 42